Original Research Article
ISSN: **3041-5357**
Journal homepage: https://diversity.researchfloor.org/

Journal of Diversity Studies

Creation of Hydrodynamic Models for Flood Disaster Mitigation Along a River Basin

Ahuchaogu, U. E.*[1], Njoku, R. E.[1], Duru, U. U.[1], Ugwu, J. O.[1], Geoffrey, O. N.[2], Ogbonna, C. G.[3], Okoroji, A. C.[1], and Onyeagoro, F. E.[1]

[1]*Department of Surveying and Geo-Informatics Federal University of Technology Owerri, Nigeria*
[2]*Department of Geomatics university of Benin, Nigeria*
[3]*Department of Urban and regional planning Federal University of Technology Owerri, Nigeria*

ABSTRACT

In contemporary times, the pace of climatic change is increasing at an alarming rate therefore the use of predictive models is increasingly gaining importance for flood impact reduction. Therefore, the aim of this research is to develop hydrodynamic models for predicting flood levels and transmission time between different locations along the lower Niger basin in Nigeria. Though several studies have been conducted on flood risk, most of them focused on spatial locations of areas exposed to risk. Notwithstanding that security of lives and property is guaranteed if time of disaster approach is accurately predicted during storm, there is dearth of research in that area of study. In this research, the geomorphology of the floodplain and Riverbed topography was mapped using SRTM DEM and bathymetric data in ArcGIS 10.4 environment. Flow predictive models and flow velocity map were developed by applying least square regression analysis and Manning's flow model using metrics of the flow route obtained by bathymetric survey and historical hydrological records. The developed models were utilized to predict water levels and transmission time of flow. The predicted variables were compared with the observed and validated after accuracy assessments. The study revealed that total transmission time of flood along the channel is approximately between 243.2 and 244.3 hours and the flow velocity along the channel falls within the range of $9.48*10^{-2}ms^{-1}$ to $1.129ms^{-1}$. It further revealed that flow velocities and transmission time between different locations along the basin varies and show correlation with the river slopes and depths.

Keywords: *Flood, Hazard, Prediction, Hydrodynamic, Models.*

Citation: Ahuchaogu, U. E., Njoku, R. E., Duru, U. U., Ugwu, J. O., Geoffrey, O. N., Ogbonna, C. G., Okoroji, A. C., and Onyeagoro, F. E. [2026]. Creation of Hydrodynamic Models for Flood Disaster Mitigation Along a River Basin. *Journal of Diversity Studies.*
DOI: https://doi.org/10.51470/JOD.2026.5.1.235

Corresponding Author: *Ahuchaogu, U. E*

E-mail Address: *udo.ahuchaogu@futo.edu.ng*

Article History: *Received 17 February 2026 | Revised 19 March 2026 | Accepted 16 April 2026 | Available Online May 20, 2026*

1.0 Introduction

Due to increase in climatic change, the use of flood predictive models is increasingly gaining importance for flood impact mitigation. In the present study, an attempt has been made to understand flow dynamics along the lower Niger basin in Nigeria by drawing inferences from statistical analysis of flood transmission using past flood hydrological data and geometries of the lower Niger River flow route. The major objective was to investigate flow dynamics along the lower Niger basin in Nigeria and develop reliable statistical models for predicting water level and flood transmission time between different locations along the basin during extreme weather. The frequency of flood occurrences and its devastating impacts on global communities, eco-environment and bio-diversity have been of great concern worldwide [1]. Flood is defined as a large amount of water covering an area that is usually dry [2]. It occurs when inflow exceeds the carrying capacity of a channel or Dam [3; 4]. Flooding has been recognized as one of the most dangerous disasters detrimental to the environment and human [5; 6].

Global annual average loss caused by floods is estimated to be 104 billion United State Dollars [7]. In recent times the rate and impacts of floods is increasing due to several factors including rising sea level, increased physical developments on flood plains etc. There is consensus within the scientific community that climatic change caused by anthropogenic activities has increased the brutality of precipitation events [8; 9; 10]. Floods by nature are complex events caused by improper development planning, climatic change and anthropogenic activities which changes river morphology [11]. Climate dynamic can change the hydrologic regime of river basins including low, high, and medium stream flows [12].

The International Panel on Climate Change (IPCC) reported that global temperatures will rise by 1.4–5.8 °C by 2100 and this will result to changes in climatic variables (rainfall, temperature, etc.) at regional and sub-catchment levels. Although flood hazard is a natural phenomenon, human modification and alteration of natural flood plains accentuates the severity of its consequences. Of all geo-hazards, flooding is the most common and costly [13].

Flood can destroy the natural eco-environment. The depletion of plants with its attendant soil erosion and loss of habitats for animals, may result to a decline in biodiversity and other environmental degradation problems [14]. Floods can result to destruction of landscape, natural habitats, bio-diversity as well as the survival strategies of human communities due to soil erosion and rapid water runoff. [15; 16]. Floods do not only damage properties and endanger the lives of human and animals but also produce other secondary effects like displacement of residents, and disruption of livelihoods as well [17]. According to [18] floods are one of the most frequent natural hazards and have led to human losses, large economic losses, the destruction of fertile land, and damages to properties and infrastructure.

Flooding has become a global phenomenon averaging four billion dollars annually in property damage alone [19]. In the period from 1963 to 1992 the world suffered from a total of 202 floods (most of which were flash floods, monsoon floods, headwater floods or landslides) with more than one million victims [20; 21]. In the year 1970 the coastal area of Bangladesh recorded one of the worst flood disasters of the 20th century with a cyclone which killed 500,000 people [22]. Within the period 1996 and 2005 several African countries were affected by a total of 290 flood disasters which left 8,183 people dead, displaced 23 million people and caused economic losses of $1.9 billion [23]. A report by the UN-HABITAT in 2010 predicted that within ten-year period (2010-2020) more than 25% of Africa's population living within 100km from the coasts will be at risk from sea level rise and coastal flooding [19; 24]. In line with this prediction, the Natal Province of South Africa experienced heavy flood caused by a record-breaking five-day rainstorm in 2009 which killed at least 400 people and left 55,000 people homeless.

In most cities of Nigeria, extreme rainfall, high urbanization rate with the attendant obstruction of streams and channel due to poor waste disposal behaviors and other human activities at flood plains have been found to constitute the major causes of floods [25]. The 2012 flood event in Nigeria was attributed to the release of water from Lagdo Dam in Cameroun and extreme weather. The resultant effect was devastation of low-lying areas along the lower Niger-Benue basin. Despite the benefits of Dams sudden release of water or its failure can result to a high magnitude of flooding in downstream areas of a basin [26].

The 2012 flood was very disastrous, affecting a total of 14 States with 1.3 million people displaced and about 431 people lost their lives. It affected most communities living within 5kilometers from the River Niger and River Benue trough. The National disaster impact assessment rating (IAR) instituted by National Emergency Management Agency (NEMA) categorized the affected areas into group A, B, C and D in descending level of damage and part of the study area falls under group A and others in group B. In 2018 and 2022 Nigeria experienced similar levels of flood disaster. These events were described as the worst in the nation's history with over 30% of the entire country completely submerged, resulting to the death of over 600 persons and displaced more than 2 million people from their homes in each episode. [27]. The 2018 and 2022 flood in Nigeria was also attributed to extreme rainfall which coincided with the period of excess water release from Lagdo Dam and Jebba Dam. When disaster of a particular magnitude occurs in a country, efforts should be made to prevent future re-occurrence or at least minimize the impact through various preventive programs and mechanisms.

For the fact that the magnitude of flood of 40-year return interval re-occurred within a space of 6 and 4 years with similar impact on the same communities implies that adequate mitigation measures have not been put in place.

Sustainability can only be achieved if there is efficient management of natural environment. In Africa, floods are among the most serious natural disasters, due to inadequate forecasting technologies [28]. As per [29], lack of good predictive capabilities is among the problems faced by disaster management agencies in this region in putting in place early warning sign and response mechanisms to tackle flooding. For example, communities along the lower Niger basin explained that the floods caught them by surprise and gave them no time to prepare, while others reported that they woke up in the morning to discover that everywhere has been toppled by flood [27].

As per [30], accurate predictions of water stages during high flow periods are fundamental to water resources management and flood control operations. Predictive models are invaluable in disaster analysis. It is never an easy task, because to develop a hydrodynamic model, the behavior of the river processes must be known from historical records. A hydrological model is a mathematical simulation of the hydrological process in a catchment. It can be used to better understand and explain hydrological dynamics [31]. In an ungauged catchment where stream flow data are lacking, the use of simulation models to generate runoff volumes and extreme flows on the intended stream from rainfall data is a necessity [32; 33]. Statistical models have proved very useful for flood impact mitigation. For example, [34] conducted flood frequency analysis of Ikpoba River catchment in Benin using Log Pearson type III distribution model. [35], also carried out flood frequency analysis of Osse River using Gumbel's distribution. Studies have shown that there is relationship between flow speed and channel geometrics. For example, [36] noted that geometric method is an alternative mode of estimating flood. Flow route geometrics are crucial parameters for alternative techniques of discharge estimation in an un-gauged river. As per [37], hydrological response from each catchment assists in flood routing vis-a-vis flood modeling and flood forecasting. [38], estimated the peak discharge of un-gauged river Kunur in Bendal river Basin during heavy flood using indirect methods with channel geometrics. Flood impacts can be mitigated or minimized by a combination of both the structural and nonstructural control measures. The structural mitigations are designed to divert flood water away from people; for example, building of retention ponds, levees, channel improvements, dams etc. [39]. Non-structural measures place people away from flood. They are designed to reduce the impact of flooding to society and economy, and include flood insurance, flood forecasting and warning schemes, building codes, land use planning and zoning, use of hydrological models etc. [39].

In the run up to any disaster, two things are of key importance to improve safety: these are the spatial component and time component. Two questions that should be of concern in this situation are: where is the disaster expected to occur and when? Spatial components determine where the disaster is likely to occur while the time component predicts the time of occurrence of disaster in space. Knowledge of time of occurrence of flood events improves safety and is of great importance for a variety of planning purposes. It allows for precautions to be taken and for people to be warned so that they can be prepared in advance to respond to flood events.

For example, farmers can remove animals from low-lying areas, the elderly and children can be relocated in advance, and emergency services can also make provisions for enough resources ahead of time to respond to disaster as it occurs. Communities, faced with flooding challenges, develop diversified resilience strategies. Although, many studies have been conducted on flood risk across the world but most of them focused on the spatial component. There is dearth of research involving the use of hydro-dynamic models for flow transmission time and river stage prediction to support flood impact reduction particularly in Nigeria therefore, this underscores the need for this study. In this work, flow transmission time and river stage hydrodynamic models have been developed using River channel's geometrics and flow historical records. These derivatives are useful for flood impact mitigation and management of future flood disasters within the study area

2.0 Material and Methods

2.1 Description of study area

The basin under consideration in this study covers a total land mass of approximately 70,959 square kilometers. It cuts across four major catchment areas along the lower Niger basin. These include Kogi, Edo, Anambra, and Delta River Niger basins. The most important hydro-geological features are River Niger and River Benue. The Niger River originates from Guinea in West Africa, runs through Mali, Niger, enters Nigeria through Niger State and extends to about 4000 km. The Benue River originates from the Adamawa Plateau of Northern Cameroon, flows west through the towns of Garoua and Lagdo reservoir, through Jimeta, Ibi and Makurdi in Nigeria before meeting the Niger River. These two Rivers formed a confluence at Lokoja, Kogi State in Nigeria before flowing southwards, dividing the basin into two wings and finally discharge into Atlantic Ocean in the southern coasts of Delta state. Geographically the study area is located between latitudes 5°.00`N and 8°.45`N, then longitudes 5°.00`E and 7°.45`E and lies within elevation range of 70m to 520m above mean sea level. Figure (1) is the location map of the study area.

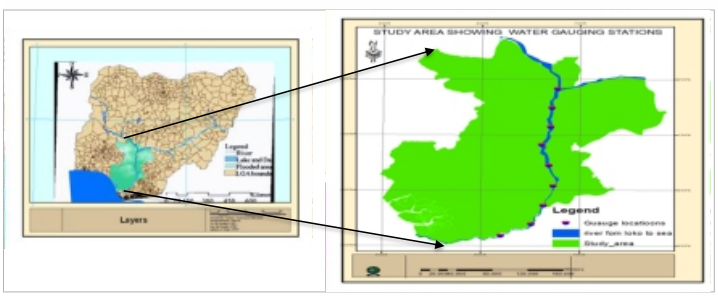

Figure 1: Location map of the study area

2.2 Data Description

The Shuttle Radar Topography Mission (SRTM) imagery of one arc seconds resolution covering the study area was acquired through the U.S. Geological Survey Earth Resources Observation and Science Center (http://earthexplorer.usgs.gov/). Other datasets include hydrological data which comprised of bathymetric (sounding) data, time series flood discharge and River stage data collected from National Inland Water Ways (NIWA) Lokoja.

These River stage data are information recorded at permanent gauging stations along the basin. Additional River stage records were collected from temporary gauging stations installed along the basin by our research group.

The permanent stations are located at Lokoja, Ajeokuta, Idah, Illushi and Onisha while the temporary stations were sited at Ogbaru, Ndokwa east, Patani and Bomadi at lower part of the basin in. Other datasets include LANSAT and IKONOS Satellite imagery of the study area collected before and during the flood episodes. These datasets have been analyzed in GIS window and the spatial extent of the river before and during the flood episodes were investigated to gain understanding of flood extent. Secondary data were collected from Ground Truthing. These include communities residing within 5kilometers from the river which were affected by the floods. This study has been carried out as per the methodology shown in Figure 2

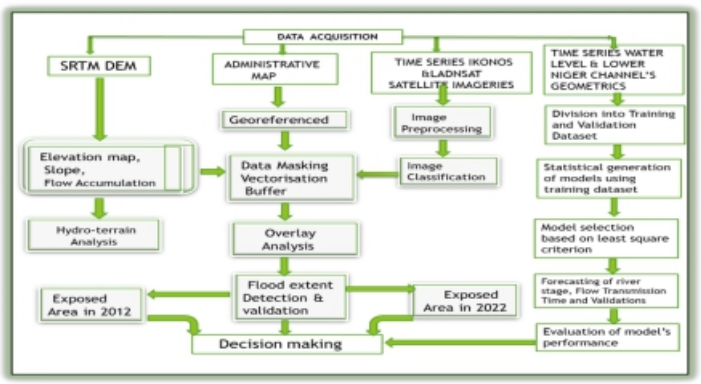

Figure 2: Methodological workflow

2.3 Flood and riverbed topography analysis

In hydrological studies the rule of thumb is that speed and direction of water flow are governed by the channel's (geometrics) configuration and shape of the surface in which it flows. Proper understanding of the terrain morphology is invaluable for prediction of the direction and speed of flowing water because water flows naturally by gravity. Satellite imageries that captured the floods were used to map the flood extents. The pre-flood imageries were used as references to determine the spatial extent of the floods through change detection analysis and later validated by ground truthing. The river layer and flood layer from each flood episode were superimposed on digital elevation model (DEM) of the study area to assess the elevation of the inundated areas and its influence on spatial spread of the floods (figure 4). Assessment of the riverbed morphology along the flow route was also carried out using bathymetric data. The reduced levels (Z) of the riverbed were processed from the chart depths (H) and reduced level (X) of the chart datum (see figure 3). The reduced hydro-terrain datasets were used for graphical assessment of the riverbed's topography (figure5a), longitudinal profile (figure 5b-c) and cross profiles (figure 5d). The area of the cross sections, the wetted perimeters and the longitudinal slopes of the Riverbed in the direction of flow at different locations were digitally measured and calculated. Progressively, the hydraulic radius at the various cross sections has been obtained as a function of the cross-sectional area and the wetted perimeter.

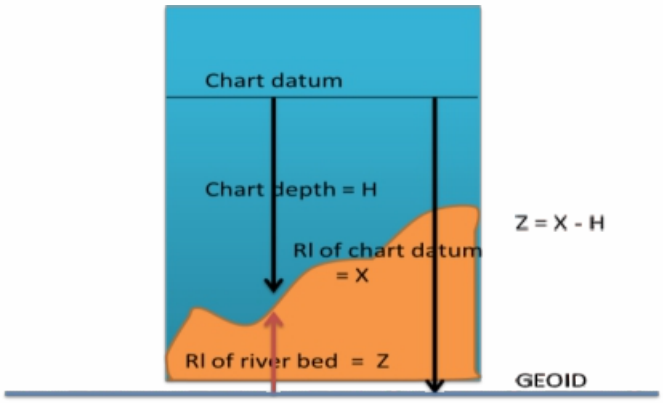

Fig 3: Reduction of the reduced level of Riverbed from chart depth to chart datum

Predictive analysis was made in two categories. The first category was based on Gauge Relation. This is an empirical hydrological modeling approach that estimates flows at downstream based on those of upstream. The idea here was to develop statistical models which are capable of estimating flood levels at downstream locations based on water level at upstream locations along the basin. Accurate river stage prediction is a crucial component in the early flood warning system and plays a key role in flood disaster mitigation. The flood warning system is a vital mitigation technique during natural disasters that can be used by river managers to make decisions before the peak flow. Two main approaches are used to establish flood prediction models. These are physics-based model and data-driven model. The physics-based model requires cross-sectional bed elevation data or digital elevation model data for establishing the simulation domain. Therefore, simulation results obtained using a physics-based model are highly dependent on the quality of topographic data. Data-driven model is based on the collection and analysis of data and does not require riverbed elevation data. It is the approach applied in river stage forecasting in this present study. The second category applied physical based approach and is based on the notion that flow speed between different locations along a River course is a function of the geometrics of the channel between these locations. Therefore, the idea here was to statistically model the relationship between flow transmission times along different river segments with the metrics of the flow route along these segments. This is done with the view of using the developed models as predictive tools during future storms.

2.4 Statistical background

Statistical background of this study is based on least square regression principle which states that of all statistical models defining relationship between variables, the one having the property that $R_1^2 + R_2^2 + R_3^2 + ---R_n^2$ is minimum is said to relate the data in least square sense and is called best fitting model [40]. Where R is the difference between the observed and the estimates. As per [40], any relationship between events (variables) in space, can be statistically modelled. The model can be used to predict any of the missing variable (unknown) provided others are known.

2.5 Predictive modelling through Gauge Relations

A total of 1080 daily water level data observed at different gauge stations along the basin collected during 2012, 2018 and 2022 flood episodes were used for this study.

540 hydro data points of these datasets captured at the gauging stations during 2012 and 2018 flood episodes were statistically combined to develop the models by applying least square regression technique while the same number of hydro-datasets collected at the same locations during 2022 flood event were used for validation. Estimation of flood levels at point B in response to flood stage at point A is the problem the model is expected to address. Both linear and nonlinear models were derived and tested using least square criterion however, this study reported and presented the models that met the least square requirement. Estimates of the observed were computed from the models developed. These estimates were compared with their observed equivalents. The residuals were fundamental to the assessment of model's result using different evaluation metrics. (For want of space, only part of the data is tabulated in appendix A and B).The goodness of fit of the models developed were assessed by applying least square criterion. The statistical models that met least square requirement were selected. Validations were carried out in relative and absolute senses to investigate the reliability of the models developed. Relative validations were made using hydrographs (figure 6) and absolute validation was made by comparison between the model's estimates and flood level at the same location captured during 2022 flood episode and accuracies of the models were calculated at 95% confidence limit.

2.6 Modeling based on channel's geometrics and time lag of transmission

This model involves statistical estimation of flow transmission time as a function of geometrics of the flow route. It is well known that speed of flowing water is a function of the character of surface in which it is flowing. During the flood episodes, communities along the basin reported that the flood caught up with them by surprise and gave them no time to prepare therefore this call for attention. Flow transmission time between different locations along the basin observed during 2012 and 2018 flood disaster was tabulated. Its variation in response to change in metrics of river flow route was assessed and statistically modelled. The channel's metrics used include average hydraulic radius and slopes of these channel segments. Hydraulic radius is the ratio of the cross-sectional area to the wetted perimeter. Hydraulic radius and slope are fundamental factors that influence flow speed along a river course. For example, Manning developed an empirical model that estimates flow speed as a function of slope and hydraulic radius (see equation 3). The observes quantities (flow transmission time (Tr) along the river segments) were made dependent (predicted) variables while average slope (S) and hydraulic radius (R) along these segments were the independent variables. Value of the constants (k's) was derived by solving the normalized equation (see equation 1). Accuracy assessment was made, and the model was further evaluated by comparing the estimated variables (time) with their observed equivalents recorded between the same locations during 2022 flood episode.

$$\begin{vmatrix} 4 & 207.663 & 2.855X10^{-4} \\ 207.663 & 11685.316 & 1.5586X10^{-2} \\ 2.855X10^{-4} & 1.5586X10^{-2} & 2.10237X10^{-8} \end{vmatrix} \begin{vmatrix} K_0 \\ K_1 \\ K_2 \end{vmatrix} = \begin{vmatrix} 120 \\ 5605.8 \\ 8.0376X10^{-3} \end{vmatrix} \quad ----(1)$$

(A^{-1} AK = A^{-1} B. Therefore, K = A^{-1} B)

2.7 Flow velocity analysis

Additional validation was made using estimated flow velocities along the basin carried out by applying Manning's flow model (see equation 2).

$$V = \frac{R^{\frac{2}{3}} S^{\frac{1}{2}}}{N} \quad \text{-------(2)}$$

Where V = Velocity,
N = Manning's Roughness Coefficient
R = Hydraulic Radius, = A/P_w
A= cross sectional area
P_w = wetted perimeter
S = Channel Slope in the direction of flow

2.8 Accuracy Assessment of Model results

Accuracy is the most important in determination of the fitness of geographic data. In statistical analysis, it is extremely helpful to use a single number to judge a model's performance. Five evaluation criteria were used for result assessment these are Nash–Sutcliffe efficiency (NSE), Coefficient of correlation (R^2), Mean absolute error (MAE), root-mean-square error (RMSE), Peak water-level error (PWE). Graphical assessment was also utilized as additional evaluation criterion (see figure 6 a, b, c, and d). NSE was initially proposed by Nash–Sutcliffe and is widely used to evaluate hydrological models. It is one of the best performance metrics for assessing the overall fit of a hydrographic record [42]. NSE is the ratio of the mean square error to the variance of observed data subtracted from unity. Its value ranges from – ∞ to 1. The closer the value of NSE to 1, the better the prediction during modeling. A negative NSE value indicates poor predictive performance. The coefficient of correlation more commonly known as R^2 quantifies the strength of the relationship between variables in a model. R^2 value ranges from 0 to 1. Zero (0) value indicates no relation, while the value of 1 indicates that the predicted values are equal to the observations. MAE indicates the number of errors obtained by a model, and the optimal value is zero. RMSE measures the average difference between values predicted by a model and the actual values. It provides an estimation of how well the model can predict the target value (accuracy). It aggregates the residuals into a single measure of predictive value. PWE is the difference between highest observed water level and highest predicted water level during the period under investigation.

$$\text{NSE} = 1 - \frac{\sum_{i=1}^{n} \left[O_i^m - O_i^p\right]^2}{\sum_{i=1}^{n} [O_i^m - \bar{O}^m]^2} \quad \text{---(3)}$$

$$R^2 = \left\{ \frac{\sum_{i=1}^{n} [O_i^m - \bar{O}^m][O_i^P - \bar{O}^P]}{\sqrt{\sum_{i=1}^{n} [O_i^m - \bar{O}^m]^2 \sum_{i=1}^{n} [O_i^P - \bar{O}^P]^2}} \right\}^2 \quad \text{--(4)}$$

$$\text{MAE} = \frac{\sum_{i=1}^{n} \left[O_i^m - O_i^p\right]}{n} \quad \text{------(5)}$$

$$\text{RMSE} = \sqrt{\frac{\sum_{i=1}^{n} \left[O_i^m - O_i^p\right]^2}{n}} \quad \text{----(5)}$$

Accuracy at 95% (CI) = RMSE x 1.96 (6)

$$PWE = O_P^P - O_P^m \quad \text{--------(7)}$$

where, n is the total number of data; O^p is the predicted water stage; O^m is the observed water stage; O_P^P, is the predicted peak water stage and O_m^P, is the observed peak water stage.

3.0 Results and Discussion

3.0.1 Result

Figure 4 a and b are the real-world views of 2012 and 2022 flood episodes respectively in the study area showing the spatial extents of floods and elevation of the affected areas. Water accumulates in areas of low-elevation making these regions more exposed to flooding. Figure 5a, b, c and d are respectively, the topography of the riverbed, 3-D riverbed's longitudinal profile, 2-D, longitudinal profile of the riverbed and part of the cross profiles of the flow route. These terrain derivatives were fundamental to generation of the channel's geo-metrics which served as input to the various statistical analysis.

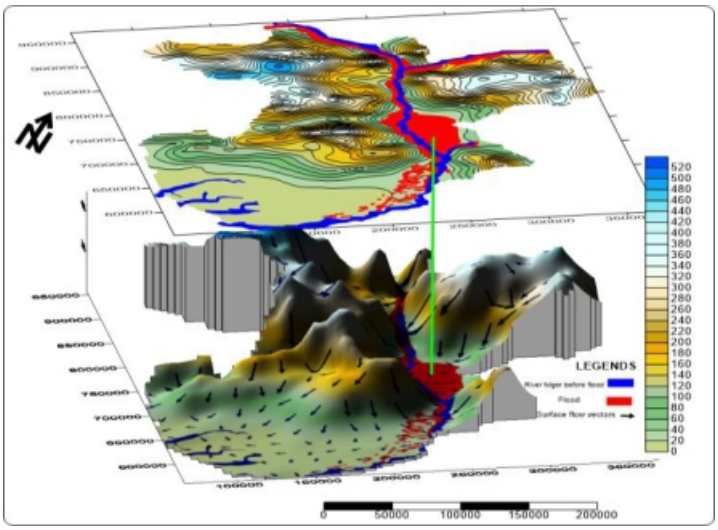

Fig 4a: Stereoscopic View of 2012 flood along the basin

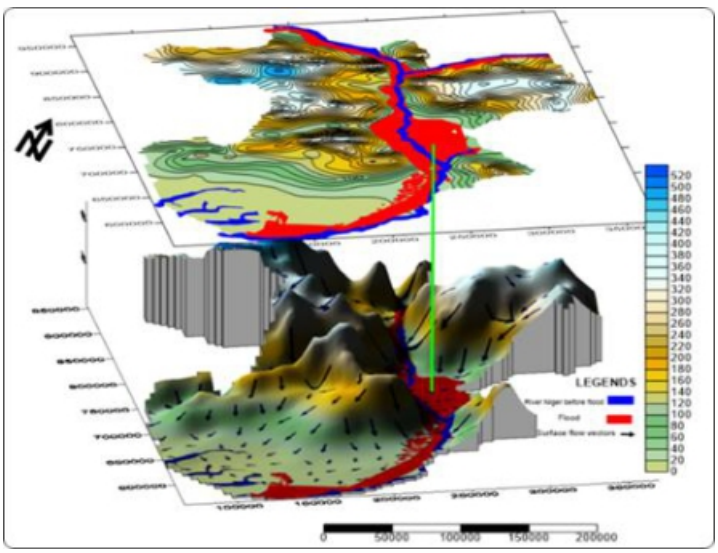

Fig 4b: Stereoscopic View of 2021flood along the bas

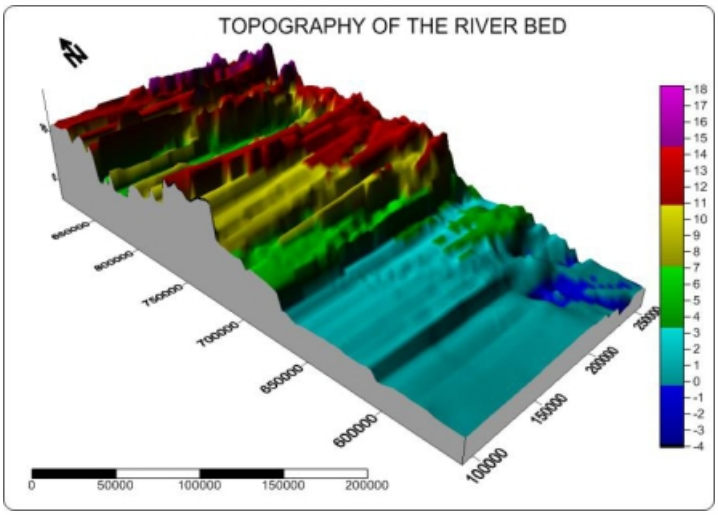

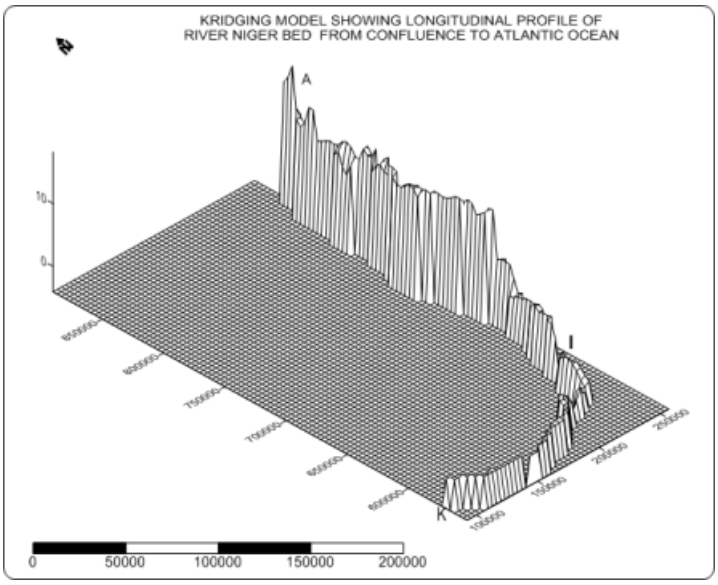

Figure5a-b: 3-D surface analysis and 3-D longitudinal profile of River Niger bed

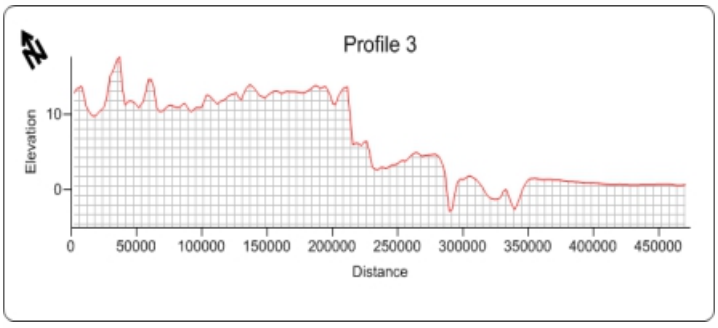

Figure 5c: 2-Dlongitudinal section of the river bed

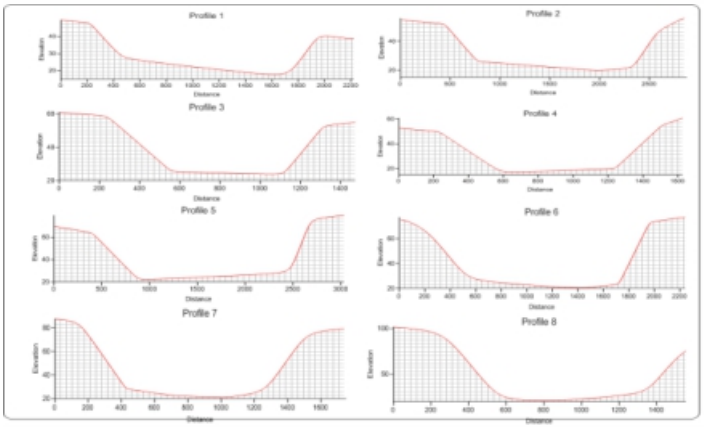

Figure 5d: Part of cross profile of the flow route

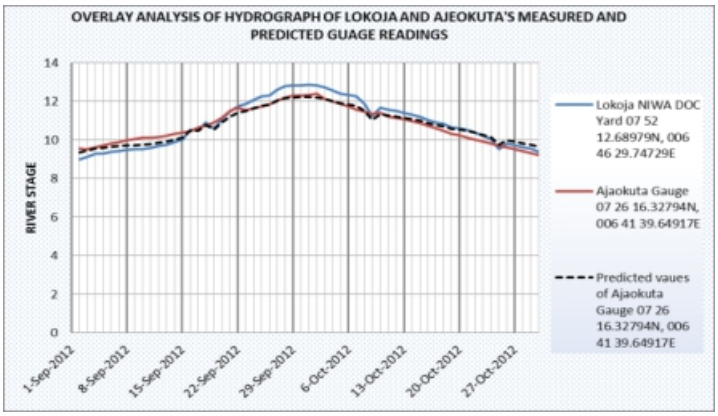

Figure 6a: Comparison of observed and forecasted river stage at Ajeokuta, and Gauging Station

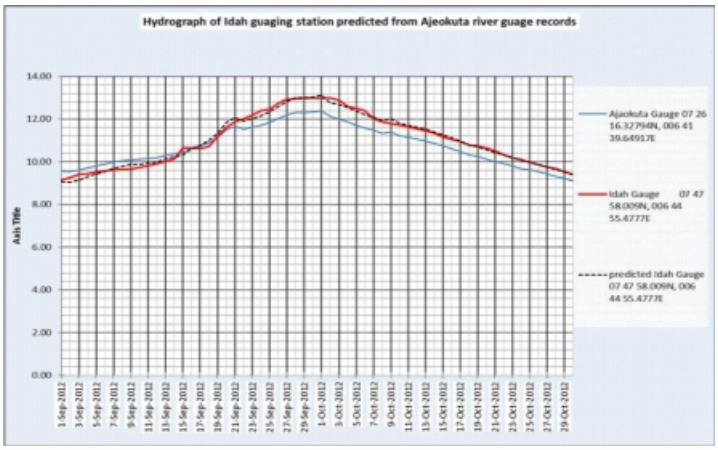

Figure 6b: Comparison of observed and forecasted river stage at Idah, gauging station

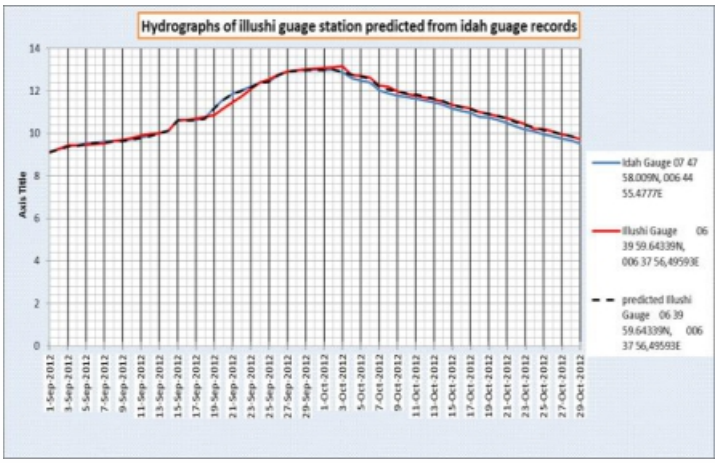

Figure 6c: Comparison of observed and forecasted river stage at Illushi gauging station

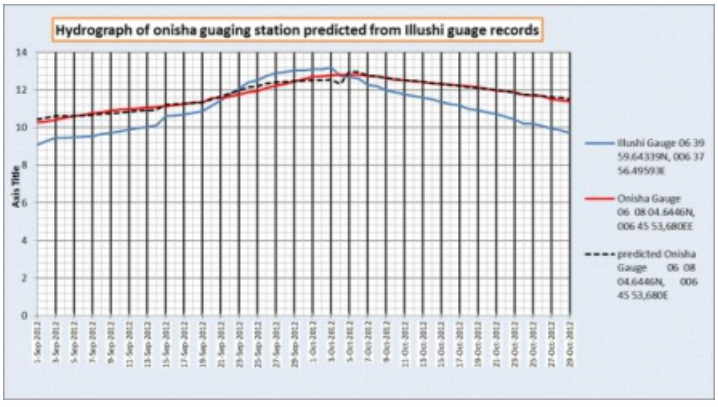

Figure 6d: Comparison of observed and forecasted river stage at Onisha gauging stati

Figure 6a, b, c, and d are hydrographs showing observed (Solid black line) and predicted (red broken lines) daily water level at four permanent gauging sites during 2012 flood period. The solid blue lines are the observed water level at the reference station. Considering the time series plots, it is evidenced that the predicted water levels approach the observed significantly.

Table 4a-11a, 4b-11b (Appendix A) and 4c -11c (Appendix B) are part of the observed and predicted river stage during 2012, 2022 and 2018 flood episode respectively showing the discrepancies between the observed and estimated water levels at stations where physical observations were made. The residuals (discrepancies) are fundamental to assessment of model's result.

3.2 Discussion

3.2.1 Topographical assessment

The Topographical models (figure 4a and 4b) revealed undulating hydro-terrain of the basin. It showed that areas of elevation ranging from 20m to 120m above mean sea level are exposed to high level of flooding. These areas are low-lying areas located within 5 kilometers from the river course. Some of the communities located within this regions are listed in the last column of table2. Below. The riverbed topography (figure5) is made of slopes of various degrees with sharp decrease in elevation from the upstream towards the downstream region of the basin. The varied slopes influences flow movement along the basin. The cross profiles (figure 5d) revealed a varying channel shape with depths varying between 50m to 100m at various locations. These attributes play significant roles in flow dynamics along the basin.

3.2.2 Analysis of river stage simulation models

The river stage predictive models and their performance indicators are shown in table 1 below. We utilized five performance indicators to determine the models' performances. This includes the coefficient of correlation (R^2), Nash–Sutcliffe efficiency, Mean absolute error (MAE), root-mean-square error (RMSE), and Peak water-level error (PWE). The coefficient of Correlation quantifies the strength of the relationship between the model's variables. A value of 1.0 indicates a perfect relationship, however this cannot be achieved because physical measurements are never perfect. The recorded R^2 values in this study are within the range of 0.9291 to 0.9905. This signifies excellent relationships between the model variables hence reliability of the estimates.

[43] and [44] have defined performance ratings for NSE. Based on their evaluation scheme, 0.75<NSE≤1 is rated very good, 0.65<NSE≤0.75 is rated good, 0.5<NSE≤0.65 is rated satisfactory, and NSE ≤0.5 is rated unsatisfactory. This study recorded NSE range of 0.8215 to 0.9959. We considered this performance to be very good based on the above rating scheme.

MAE and RMSE are indicators showing the number of errors obtained by a model. Perfect fit for these variables is zero, however, this can never be obtained since every geophysical measurement is exposed to certain level of insecurity. Based on the rule of thumb, RMSE values between 0.2 and 0.5 shows that the model can predict the data accurately. RMSE range of 0.0657 to 0.4159 resulting from this study and the values of MAE as shown in table1 indicate that the models' estimates are reliable.

Peak water level is of significant concern to water resources planners and decision-makers. This is because pre- knowledge of peak flow is very crucial for preparing for emergency response and other impact reduction measures. Peak water error (PWE) is the difference between the observed and predicted peak water level. PWE determined at the various stations are between the range of 0.01m to 0.75m. This shows that the models were able to accurately predict the highest water levels.

3.2.3 Flow Time Prediction

Result of flow transmission time analysis is presented in table2 below. It captured the observed and predicted time of flow transmission during the flood episodes. Accurate timing of the incoming flow is required to prepare for mitigation measures. We evaluated flow transmission time predictive performance using four evaluation metrics (see table 3). The predictive model (equation 8) was trained using data collected during 2012 and 2018 flood event and validated using data collected during 2022 flood episode. The performance evaluators, which include R2, NSE, MAE and RMSE, showed values ranging from 0.9996 to 0.9999, 0.9996 to 0.9998, 0.0985 to 0.1238 and 0.1935 to 0.2168 respectively. These statistics indicate excellent performance as per the standard we utilized in section 3.2.2 above. The observed total time of flood transmission ($T_{ob}TTr$) along the basin during 2012, 2018 and 2022 are 244.2 hours, 244 hours, and 244.3 hours respectively and the predicted equivalent (T_pTTr) is 243.2 hours. More details can be seen in table 2 below.

$$T = 0.72617699*10^{2} - 4.816589*10^{-1}R - 2.4675325*10^{5}S \quad -- (8)$$

Table 1: Evaluation metrics of river stage predictive models

S/N	Predictive model	Guaging station	YEAR	R^2	NSE	MAE	RMSE	PWE	ACCURACY AT 95% (CI)
1	$Y_A = 0.6955XL+3.347$	Ajeokuta	2012 2018 2022	0.9862	0.9862 0.9877 0.9805	$55x10^{-5}$ $48x10^{-4}$ $37x10^{-2}$	0.1136 0.1322 0.1417	0.06 0.07 0.25	0.2227 0.2591 0.2777
2	$Y_{ID} = 1.4263X_A - 4.5519$	Idah	2012 2018 2022	0.9865	0.9865 0.9782 0.9572	$76x10^{-5}$ $56x10^{-4}$ $20x10^{-1}$	0.1615 0.2217 0.3217	0.02 0.24 0.33	0.3165 0.4345 0.6305
3	$Y_{IL} = I,0025X_{1D} - 0.0467$	Illushi	2012 2018 2022	0.9894	0.9894 0.9879 0.9887	$17x10^{-5}$ $15x10^{-3}$ $15x10^{-3}$	0.1458 0.1412 0.1466	0.20 0.16 0.14	02843. 0.2768 0.2783
4	$Y_{ON} = 0.5223X_{IL} + 5.6696$	0nisha	2012 2018 2022	0.9571	0.9571 0.9577 0.9429	$41x10^{-5}$ $52x10^{-4}$ $68x10^{-2}$	0.1566 0.1891 0.1975	0.25 021 0.10	0.3069 0.3882 0.3871
5	$Y_{OG} = 1.4127X_{ON} – 5.607$	Ogbaru	2012 2018 2022	0.9905	0.9905 0.9882 0.9856	$39x10^{-4}$ $53x10^{-3}$ $92x10^{-2}$	0.1019 0.1231 0.1364	0.08 0.10 0.17	0.1997 0..2413 0.2413
6	Y_{ND} $0.9182X_{OGB} – 0.0544$	Ndokwa	2012 2018 2022	0.9834	0.9834 0.9966 0.9959	$55x10^{-4}$ $51x10^{-3}$ $46x10^{-2}$	0.1241 0.1123 0.0652	0.01 0.08 0.09	0.2432 0.2201 0.1278
7	$Y_{PA} = 1.0264X_{ND} - 1.1164$	Patani	2012 2018 2022	0.9291	0.9291 0.9192 0.9062	$31x10^{-4}$ $23x10^{-3}$ $14x10^{-1}$	0.2733 0.2241 0.3472	0.52 0.26 0.75	0.5356 0.4392 0.6805
8	$Y_{BU} = 0.8272X_{PA} + 1.582$	Burundi	2012 2018 2022	0.8270	0.8270 0.8337 0.8215	$33x10^{-4}$ $43x10^{-3}$ $54x10^{-2}$	0.3384 0.3611 0.4159	0.09 0.21 0.22	0..6632 0.7077 0.8152

Table 2: Time lag of flow between various locations along lower Niger basin.

Location from	Location to	Length of River Segment (m)	R_{avr} (m)	S_{avr}	T_{obs} in 2012 (hrs)	T_{obs} in 2018 (hrs)	T_{obs} in 2022 (hrs	T_{Est} (hrs)	R_1	R_2	R_3	Communities 5km from the River
Lokoja 07 52 12.698N 06 46 29.747E	Ajeokuta 07 26 16.32N 06 41 39.64E	46907	61.024	$7.97x10^{-5}$	24.00 24hr 00m	23.90 23hr 54m	23.70 23hr 42m	23.56 23hr 34m	0.44 26min	0.34 20m	0.14 8min	Ganaja, Shintaku,jingbe, Icheu, koji, Baraga, Egbo, Eroko, Kuroko, Geregu etc
Ajeokuta 07 26 16.32N 06 41 39.64E	Idah 07 47 58.010N 06 44 55.478E	46899	60.816	$7.88x10^{-5}$	24.00 24hr 00m	23.88 23hr 53m	24.00 24hr 00m	23.88 23hr 53m	0.12 7min	0.00 00min	0.12 7min	0guro, Itobe, Olukubu, Okekenji, Gbake, Oyele, Anomogbo
Idah 07 47 58.010N 06 44 55.478E	Illushi 06 39 59.643N, 06 37 56.495E	46897	59.941	$7.72x10^{-5}$	24.00 24hr 00	24.00 24hr 00m	23.90 23hr 54m	24.28 24hr 16m	-0.28 -16min	-0.28 -16min	-0.38 -22min	Isara, odeke, Okuokata,Ofugbo, Upeko, Akie, EpeUdiaba, ogwujibo, Ugaine,etc
Illushi 06 34 59.981N 05 35 21.238E	Onisha 06 08 04,6446N 06 45 53.680E	46901	25.882	$4.94x10^{-5}$	48.00 48hr 00m	47.90 47hr 54m	47.90 47hr 54m	47.96 47hr 58m	0.04 2min	-0.06 -4min	-0.06 '4min	Odumomo, Oduchala, Adagwo, Odekpe, Illah, Ogene, Imiku, Umuzie,
Onisha 06 08 04,6446N 06 45 53.680E	Ogbaru 06 38 51.505N 05 49 58.477E	46899	39.565	$14.24x10^{-5}$	18.40 18hr 24m	18.39 18hr 23m	18.50 18hr 30m	18.42 18hr 25m	-0.02 -1min	-0.03 -2min	0.08 5min	AkiliOgidi, Akili -Ozizor,Amiyi, Atani, Mputu,, Odekpeetc
Ogbaru 06 38 51.505N 05 49 58.477E	Ndokwa East 06 34 59.981N 05 35 21.238E	46905	35.772	$12.98x10^{-5}$	23.30 23hr 18m	23.32 23hr 19m	23.40 23hr 24m	23.36 23hr 22m	-0.06 -4min	-0.04 -3min	0.04 2min	Odekpe, Ogwu-AmochaAboh, Ashakaetc
Nowa , E 06 34 59.981N 05 35 21.238	Patani 06 22 14.841N 05 15 53.021E	46909	34.242	$12.02x10^{-5}$	26.50 26hr 30m	26.51 26hr 31m	26.60 26hr 36m	26.46 26hr 28m	0.04 2min	0.05 3min	0.14 8min	Aven, OgborAdobor Bulu – Anyiama, Uduophoni, Ogolomo
Patani 06 22 14.841N 05 15 53.021E	Bomadi 06 04 9.38N 05 05 4.98E	46899	17.558	$3.32x10^{-5}$	56.00 56hr, 00m	55.93 55hr 56m	56.00 56hr 00m	55.97 55hr 58m	0.03 2min	-0.04 -2min	.03m 2min	NONE

Note: Location from = Location of the gauging station at the upstream along a river l; Location to = Location of the gauging station at the downstream along a river ; R_{avr} = average hydraulic radius of a particular river segment; S_{avr} = average slope of the river bed along a particular length of the river in the direction of flow; T_{obs} = Observed time lag of flood transmission between two locations along the river; T_{Est} = Predicted time lag of flood transmission between two locations along the river; R_1= difference between observed and predicted time lag of flow transmission between various location in 2012 R_2 = difference between observed and predicted time lag of flow transmission between various location in 2018 . R_3 = difference between observed and predicted time lag of flow transmission between various location in 2022 and estimated

Table 3: Evaluation of Model performance in flow transmission time prediction

YEAR	R^2	NSE	MAE	RMSE	Accuracy at 95%(CI)	$T_{ob}TT_r$	T_pTT_r
2012	0.9998	0.9997	0.1238	0.2168	0.4249	244.2 Hours	
2018	0.9999	0.9998	0.0988	0.1937	0.3797	244 Hours	243.21Hours
2022	0.9996	0.9996	0.0985	0.1935	0.3792	244.3 Hours	

Figure 7 below shows the flow velocity map generated by applying Manning's flow model which was used for further validation. The study revealed that flow velocity along the channel falls within the range of $9.48*10^{-2}ms^{-1}$ to 1.129ms. High flow velocities were observed in areas of low transmission time and vice versa and these show correlation with the slopes and river depth.

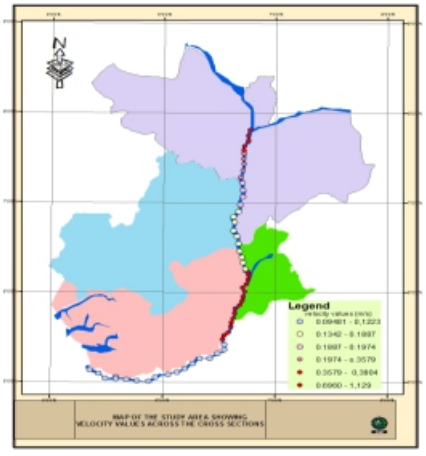

Figure 7: Flow velocity map along the basin

4.0 Conclusion

Flood emergency management agencies (both public and private) in this region are often reactive rather than proactive in response to crises. They are usually not concerned with the fundamental issues of mitigations or impact reduction measures. One of the primary reasons for this is lack of effective prediction of events. Flood cannot be prevented but its impacts can be reduced if adequate preparations are made. Although flood risk analysis has been conducted in many cities around the globe, most of them focused on spatial components. This has to do with the determination of areas or locations under different flood risk potential levels. However, none of these studies (especially in Nigeria) incorporated predictive models. As a result, many communities along the Lower Niger Basin in Nigeria are adversely affected during extreme climatic condition. Accurate and reliable flow prediction of river dynamics during storms is essential for flood control, mitigation of flood hazard, evacuation of people from flood hazard areas etc. Considering the high records of flooding events along Lower Niger Basin, determination of the hydrological character of the river was essential.

Thus, identification of such hydrological behaviors benefits modelers with an efficient tool to predict the water level and flow transmission time and so as to reduce potential damages of flood events therefore this is the rationale for this study. In this study Morphology of the basin and riverbed was investigated and displayed using different visual format and reliable hydrodynamic models for river stage and flow transmission time prediction have been developed. Least square regression analysis was used to model the relationship between hydrological variables along the basin and most suitable models were selected by applying least square criterion. The models developed were validated, graphically and statistically to verify their predictive capabilities. Evaluation metrics which include R2, NSE, MAE , RMSE and PWE were applied to compare the predicted results with the observed data and significant level of agreement was observed. These models are invaluable for reliable water level and flow transmission time forecasting along the basin without relying totally on observations from gauging stations especially in areas lacking river stage measuring instruments. The results of the analysis have direct application in the formation of policies on disaster management, flood risk assessment and reduction along the Basin in future

References

1. Destaw, K. and Assayew, N. (2025). Flood monitoring and damage assessment in agricultural field using Sentinel-1 SAR data in Gumara river catchment, Blue Nile basin, Environmental Systems Research, 14(32) pp1-19 https://doi.org/10.1186/s40068-025-00427-1
2. Olajuyigbe, E. A. (2012). Mapping and analysis of 2012 flood disaster in Edo State using geospatial technique. Journal of environmental sciences. 6 (5), pp 32-44.
3. Emmanuel, U. A., Aniekan, E. (2017). River inundation and flood hazard zonation in Edo State using geospatial technique. The International Journal of Engineering and Science. 6, (8) PP48-59
4. Aldardasawi AM, Eren B (2021) Floods and their impact on the environment. Acad Perspective Procedia 4(2):42–49
5. Masoud, M., Amini, M. H., Maghsoudi, S. F., & Alipour, S. (2020). Spatial multicriteria decision analysis for flood susceptibility mapping in Talesh Coastal Plain, Iran. International Journal of Environmental Research, 14(2), 193–208
6. Kurapati, P.V., Babu, A., Pyla, K.R, Nsr, P., Mandla, V.R.B (2023) Flood mapping and damage assessment using Sentinel – 1 & 2 in Google Earth engine of Port Berge & Mampikony Districts, Sophia Region, Madagascar. Adv Scalable Intell Geospatial Analytics: Challenges Appl 1:288–289 https://doi.org/10.1201/9781003270928-20
7. Sehrish, K, Q. A, Muhammad Z. A, Syed, A. M. A, Ahsan, U/ B., Muhammad, S. B (2021). Socioeconomic determinants of climate change adaptations in the flood-prone rural community of Indus Basin, Pakistan. Environmental Development. V37. Available online at https://doi.org/10.1016/j.envdev.2020.100603
8. Lyu, H., Wang, G., Shen, J., and Lu, L. (2016). Analysis and GIS mapping of flood hazard in Guangzhou china. Water journal (8)447 pp1-17
9. Al-Quraishi, A. M., & Babel, M. S. (2021). Flood hazard mapping in Iraq using multicriteria decision analysis and machine learning techniques. The Egyptian Journal of Remote Sensing and Space Science, 24(2), 339–353.
10. Christo, G., Loannis, T., Anthi-Irini, V., and George, P. K. (2022). Flood risk assessment and flow modeling of the Stalos Stream area. Journal of hydro informatics. 24 (3) pp 677-696
11. Aramburú-Paucar, J. M., Martínez-Capel, F., Puig-Mengual, C. A., Muñoz-Mas, R., Bertagnoli, A., & Tonina, D. (2024). A large flood resets riverine morphology improve connectivity and enhances the habitats of a regulated river. Science of The Total Environment, 919, 170717. https://doi.org/10.1016/j.scitotenv.2024.170717
12. Alodah, A., Seidou O (2019) Assessment of climate change impacts on extreme high and low flows: an improved bottom-up approach. Water 11:1236. https://doi.org/10.3390/w11061236
13. Emmanuel, U. A., Ojinnaka, O.C., Baywood, C.N .(2015). Flood Hazard analysis and damage assessment of 2012 Flood in Anambra State using GIS and remote sensing approach. American Journal of Geographic Information System, 4(1): pp38-51
14. Benefit O (2024) The Impacts of Flooding on the Depletion and Dispersal of Plants. Greener Journal of Agronomy, Forestry and Horticulture Vol. 8(1), pp. 1-5. https://gjournals.org/GJAFH
15. Mahé, G., Liénou, G., Olivry, J. C., Orange, D., Ardoin-Bardin, S., & Servat, E. (2013). The impact of land use change on soil water holding capacity and river flow modeling in a tropical humid and semi-arid region. Hydrology and Earth System Sciences, 17(6), 2253-2275
16. Alexis D, Ezechiel K. (2025). Impact of Floods on Biodiversity and Resilience of Affected Local Communities in the Far North Region of Cameroon. HAL Open Science. https://hal.science/hal-05004422v1
17. Nji, T. M., Balgah, R. A., & Vubo, E. Y. (2019). Coping with flood hazards in Cameroon: The role of community-based strategies. Sociology International Journal, 3(5)pp372382. DOI:10.15406/sij.2019.03.00202
18. Masoud, M., Amini, M. H., Maghsoudi, S. F., & Alipour, S. (2020). Spatial multicriteria decision analysis for flood susceptibility mapping in Talesh Coastal Plain, Iran. International Journal of Environmental Research, 14(2), 193–208 *(Note: This is a duplicate of reference #5)*
19. Nwilo, P.C. (2012). Survey practice in the Nigerian contemporary society. Paper presented on the occasion of the opening and dedication of 'Surveyors House' of Nigerian Institution of Surveyors (NIS), Enugu State Branch.
20. Kwak, Y. and Kondoh, A. (2008). A Study on the Extraction of Multi-Factor Influencing Floods from RS Image and GIS Data: A Case Study in
21. Ahuchaogu U. E., Ojinnaka O. C., Njoku R. N. and Baywood C. N. (2021) Earth Observation System-Based Impact Assessment of 2012 Flood in Delta State Nigeria. Civil and Environmental Research. 12, (9)79-86
22. Ikusemoran, M., Anthony, D. and Maryah, U. M.(2013). GIS based assessment of flood risk and vulnerability of communities in the Benue floodplains, Adamawa State. Nigeria. Journal of Geography and Geology. 5(4) pp148-160
23. Satterthwaite, D., Huq, S., Pelling, M., Reid, H. and Lankao, P. (2007). Adapting to climate change in urban areas. International Institute for Environment and Development, London.: http://pubs.iied.org/pdfs/10549IIED.pdf.
24. Ejikeme, J.O., Igbokwe, J.I., Ojiako, J.C.,Emengini, E.J., and Aweh, D.S. (2015). Modelling the impact of flooding using geographic information system and remote sensing. International Journal of Technical Research and Applications. 3(4) , PP. 67-72
25. Knuth, R. (2025) GIS-Based Flood Risk Mapping and Disaster Preparedness. J Remote Sens GIS (14) pp 1-2 DOI: 10.35248/2469-4134.24.14.390,
26. Anu, A., Utsav, B., Vishnu, P. P. and Pawan, K. B (2024) Downstream impacts of dam breach using HEC-RAS: a case of Budhigandaki concrete arch dam in central Nepal. Environmental Systems Research Environmental Systems Research 13 (37) 1-16 https://doi.org/10.1186/s40068-024-00358-3

27. Ominabo, W. D. (2022). 2022 Flood: A tragedy foretold. https://www.thisdaylive.com/index.php/2022-flood-a-tragedy-foretold/ Accessed 23 November 2022
28. Ejigu, N. F. (2016). Flood Risk Analysis With Regards To Crop Yield in Upper Awash River Basin, Ethiopia (Case Study of Teji River)
29. Ogbonna, C. G. Eleazu, E. I., Obinka, A. N., and Ukpabi, J. I. (2016). Features of Urban Drainage Systems in Aba, Nigeria. Asian Journal of Science and technology. 07(11), pp.3922 – 3931
30. Wen-Cheng, L and Chuan-En, C (2014) Enhancing the Predicting Accuracy of Water Stage Using physical based Model and Artificial neural network and artificial Neural Network Genetic Algorithm in a River System, Water 6(6) pp1642-1661
31. Haan, C. T., Johnson, H. P., and Brakensiek, D. L. (1982). Hydrologic modeling of small watershed. St Joseph American society of Agricultural Engineers (ASAE). 13(2), pp123-124
32. Salau1, O. B., Salaudeen, A., Gana, B. Zubairu, I., Musa, S. I (2021). Assessment of a New Dam Site for Water Supply Potential in Bauchi Metropolis, Nigeria. Nigerian Journal of Technological Development 18 (4) pp312-321
33. Salaudeen, A.; S. Shahid, T. Ismail, E.-S. Chung, M. Mohsenipour and X.-J. Wang (2016). Prediction of Flow Duration Curve in Ungauged Catchments using Gene Expression Programming. Procedia Eng. 154: 1431-1438
34. Izinyon, O.C., and Igbinoba G. E. (2011). Flood frequency analysis of Ikpoba River catchment at Benin city using log Pearson Type III distribution. Journal of Emerging Trends in Engineering and Applied Sciences (JETEAS) 2 (1), pp 50-55
35. Okonofua. (2013). Flood frequency analysis of Osse River using Gumbel's distribution. Journal Civil and Environmental Research. 3(10), pp 55-59
36. Bhatt, V.K. and Tiwari, A.K (2008). Estimation of peak stream flows through channel geometry. Hydrological sciences Journal. 53(2) PP 401-403
37. Anupam, K. S., Sudhakar, S., Utkarsh, V., and Arun, K. S. (2011). Estimating Hydrological Parameters in Ungauged Basins Using Field Measurements and GIS. National Symposium Empowering Rural India through Space Technology November 9-11, 2011. Available at Bhopal https://www.researchgate.net/publication/257866377
38. Suvendu, R. and Biswaranjan, M. (2013). Estimation of peak flood discharge for an Ungauged River: A case study of the Kunur River, West Bengal. Geography Journal. 2013 pp 1-11. DOI:10.1155/2013/214140
39. ESCAP/UN. (1991). Manual and Guide Line for Comprehensive Flood Loss Prevention and Management
40. ESCAP (1991). Manual and Guidelines for comprehensive flood loss prevention and management. https://repository.unescap.org
41. Murray, R. P. and Larry, J. S. (2008). Theory and Problems of Statistics, 4th Edition, Schum's Outline Series, McGraw-Hill, USA, pp316 – 357
42. Hakan, T. and Martin J. B (2018), Simulation and Forecasting of stream Flow using machine learning Models Couple with Base Flow Seperation. Journal of Hydrology 564 (2018) pp266-282
43. Pan, T., Wu, S., Dai, E and Liu, Y. (2013) Estimating the daily global daily radiation spatial distribution from diurnal temperature ranges over the Tibetan plateau in China, Applied Energy, 107, 384-393
44. Cho, J., Bosch, D., Vellidis, G. Lawrance, r. and Strickland T (2012). Multi-site evaluation of hydrology component of SWAT on coastal plain of south west Geogia. Hydrological Process, 27(12), 1691-1700

APPENDIX (A1)

Table 4a: Part of observed and forecasted water levels at Ajeokuta station in 2012

Date	Ajeokuta gauge readings in 2012 (m)	Estimated water Level (m)	Residuals	Date	Ajeokuta gauge readings in 2012 (m)	Estimated water Level (m)	Residuals	Predictive Model
1-Sep-2012	9.56	9.6	-0.04	8-Sep-2012	10.05	9.95	0.1	$YA = 0.6955X_L + 3.347$ (YA= estimated water level at Ajeokuta. XL= observed water level at Lokoja)
2-Sep-2012	9.53	9.69	-0.16	9-Sep-2012	10.11	9.96	0.15	
3-Sep-2012	9.60	9.79	-0.19	10-Sep-2012	10.12	10.01	0.11	
4-Sep-2012	9.72	9.81	-0.09	11-Sep-2012	10.16	10.07	0.09	
5-Sep-2012	9.80	9.87	-0.07	12-Sep-2012	10.20	10.13	0.07	
6-Sep-2012	9.89	9.9	-0.01	13-Sep-2012	10.31	10.21	0.1	
7-Sep-2012	9.99	9.93	0.06	14-Sep-2012	10.37	10.3	0.07	

Note: Date = date of gauge observation; Gauge reading = observed flood level; Estimated water level = water level estimated from the statistical model; Residuals = difference between the observed and estimated water level: Predictive model = mathematical model from which the estimates were derived

Table 4b: Part of observed and forecasted water levels at Ajeokuta station in 2022

Date	Ajeokuta gauge readings in 2022 (m)	Estimated water level (m)	Residuals	Date	Ajeokuta. gauge readings in 2022 (m)	Estimated water level (m)	Residuals
5-Sep-2022	9.52	9.6	-0.08	12-Sep-2022	10.04	9.95	0.09
6-Sep-2022	9.48	9.69	-0.21	13-Sep-2022	10.10	9.96	0.14
7-Sep-2022	9.55	9.79	-0.24	14-Sep-2022	10.11	10.01	0.1
8-Sep-2022	9.69	9.81	-0.12	15-Sep-2022	10.15	10.07	0.08
9-Sep-2022	9.77	9.87	-0.1	15-Sep-2022	10.19	10.13	0.06
10-Sep-2022	9.86	9.9	-0.04	17-Sep-2022	10.31	10.21	0.1
11-Sep-2022	9.97	9.93	0.04	18-Sep-2022	10.37	10.30	0.07

Note: Date = date of gauge observation; Gauge reading = observed flood level; Estimated water level = water level estimated from the statistical model; Residuals= difference between the observed and estimated water level: Predictive model = mathematical model from which the estimates were derived

Table 5a: Part of observed and forecasted water levels at Idah station in 2012

Date	Idah Gauge Reading in 2012 (m)	Estimated Water level (m)	Residuals	Date	Idah Gauge Reading	Estimate	Residuals	Predictive Model
1-Sep-2012	9.14	9.08	0.06	8-Sep-2012	9.64	9.78	-0.14	$Y_{ID} = 1.4263X_A - 4.5519$ (Y_{ID}= estimated water level at Idah, X_A= observed water level at Ajeokuta
2-Sep-2012	9.26	9.04	0.22	9-Sep-2012	9.66	9.87	-0.21	
3-Sep-2012	9.41	9.14	0.27	10-Sep-2012	9.73	9.88	-0.15	
4-Sep-2012	9.44	9.31	0.13	11-Sep-2012	9.81	9.94	-0.13	
5-Sep-2012	9.52	9.42	0.10	12-Sep-2012	9.90	9.99	-0.09	
6-Sep-2012	9.57	9.55	0.02	13-Sep-2012	10.02	10.15	-0.13	
7-Sep-2012	9.61	9.69	-0.08	14-Sep-2012	10.14	10.24	-0.10	
Note: Date = date of gauge observation; Gauge reading = observed flood level; Estimated water level = water level estimated from the statistical model; Residuals = difference between the observed and estimated water level: Predictive model = mathematical model from which the estimates were derived								

APPENDIX (A2)

Table 5b: Part of observed and forecasted water levels at Idah station in 2022

Date	Idah Gauge Reading (m)	Estimated water leve(m)	Residuals	Date	Idah Gauge Reading(m)	Estimated water level(m)	Residuals
5-Sep-2022	9.12	9.08	0.04	12-Sep-2022	9.68	9.78	-0.09
6-Sep-2022	9.26	9.04	0.22	13-Sep-2022	9.70	9.87	-0.15
7-Sep-2022	9.42	9.14	0.29	14-Sep-2022	9.78	9.88	-0.092
8-Sep-2022	9.46	9.31	0.15	15-Sep-2022	9.87	9.94	-0.06
9-Sep-2022	9.55	9.42	0.12	15-Sep-2022	9.97	9.99	-0.01
10-Sep-2022	9.60	9.55	0.05	17-Sep-2022	10.11	10.15	-0.03
11-Sep-2022	9.65	9.69	-0.04	18-Sep-2022	10.24	10.24	0.01
Note: Date = date of gauge observation; Gauge reading = observed flood level; Estimated water level = water level estimated from the statistical model; **Residuals**= difference between the observed and estimated water level: Predictive model = mathematical model from which the estimates were derived							

Table 6a: Part of observed and forecasted water levels at at Illushi station in 2012

Date	Illushi Gauge Reading (m)	Estimated water level (m)	Residuals	Date	Illushi Gauge Reading	Estimated water level	Residuals	Predictive model
1-Sep-2012	9.09	9.12	-0.03	8-Sep-2012	9.65	9.62	0.03	Y_{IL}= I,0025X_{1D} -- 0.0467. (Y_{IL}= Estimated water level at Illushi, X_{ID}= Measured water Level at Idah
2-Sep-2012	9.27	9.24	0.03	9-Sep-2012	9.71	9.64	0.07	
3-Sep-2012	9.45	9.39	0.06	10-Sep-2012	9.8	9.71	0.09	
4-Sep-2012	9.44	9.42	0.02	11-Sep-2012	9.9	9.79	0.11	
5-Sep-2012	9.47	9.50	-0.03	12-Sep-2012	9.98	9.88	0.1	
6-Sep-2012	9.51	9.55	-0.04	13-Sep-2012	10.02	10.00	0.00	
7-Sep-2012	9.54	9.59	-0.05	14-Sep-2012	10.12	10.12	-0	
Note: Date = date of gauge observation; Gauge reading = observed flood level; Estimated water level = water level estimated from the statistical model; **Residuals;** difference between the observed and estimated water level: Predictive model = mathematical model from which the estimates were derived								

Table 6b: Part of observed and forecasted water levels at Illushi station in 2022

Date	Illushi Gauge Reading (m)	Estimated water level(m)	Residuals	Date	Illushi Gauge Reading (m)	Estimated water level (m)	Residuals
5-Sep-2022	9.14	9.12	0.02	12-Sep-2022	9.68	9.62	0.06
6-Sep-2022	9.31	9.24	0.07	13-Sep-2022	9.74	9.64	0.10
7-Sep-2022	9.49	9.39	0.10	14-Sep-2022	9.83	9.71	0.12
8-Sep-2022	9.48	9.42	0.06	15-Sep-2022	9.93	9.79	0.14
9-Sep-2022	9.52	9.50	0.02	15-Sep-2022	10.01	9.88	0.13
10-Sep-2022	9.55	9.55	0.00	17-Sep-2022	10.04	10.00	0.04
11-Sep-2022	9.58	9.59	-0.01	18-Sep-2022	10.14	10.12	0.02
Note: Date = date of gauge observation; Gauge reading = observed flood level; Estimated water level = water level estimated from the statistical model; **Residuals**= difference between the observed and estimated water level: Predictive model = mathematical model from which the estimates were derived							

APPENDIX (A3)

Table 7a: Part of observed and forecasted water levels at Onisha station in 2012

Date	Onisha Gauge Reading (m)	Estimated water level(m)	Residuals	Date	Onisha Gauge Reading (m)	Estimated Water level. (m)	Residuals	Predictive model
01-Sep-12	10.23	10.42	-0.19	08-Sep-12	10.8	10.72	0.08	YO N = 0.5223XIL + 5.6696Y_{ON} = Estimated water level at Onisha, X_{IL} = Measured Water level at Illushi
02-Sep-12	10.38	10.52	-0.14	09-Sep-12	10.84	10.75	0.09	
03-Sep-12	10.48	10.61	-0.13	10-Sep-12	10.89	10.79	0.1	
04-Sep-12	10.59	10.61	-0.02	11-Sep-12	10.95	10.85	0.1	
05-Sep-12	10.64	10.62	0.02	12-Sep-12	10.99	10.89	0.1	
06-Sep-12	10.65	10.64	0.01	13-Sep-12	11.05	10.91	0.14	
07-Sep-12	10.69	10.66	0.03	14-Sep-12	11.09	10.96	0.13	
Note: Date = date of gauge observation; Gauge reading = observed flood level; Estimated water level = water level estimated from the statistical model; **Residuals=** difference between the observed and estimated water level: Predictive model = mathematical model from which the estimates were derived								

Table 7b: Part of observed and forecasted water levels at Onisha station in 2022

Date	Onisha Gauge Reading m)	Estimated water Level (m)	Residuals	Date	Onisha Gauge reading (m)	Estimated water level (m)	Residuals
05-Sep-22	10.26	10.42	-0.16	12-Sep-22	10.82	10.72	0.11
06-Sep-22	10.32	10.52	-0.2	13-Sep-22	10.89	10.75	0.14
07-Sep-22	10.42	10.61	-0.19	14-Sep-22	10.95	10.79	0.15
08-Sep-22	10.52	10.61	-0.09	15-Sep-22	10.98	10.85	0.13
09-Sep-22	10.6	10.62	-0.02	15-Sep-22	11.02	10.89	0.13
10-Sep-22	10.67	10.64	0.03	17-Sep-22	11.07	10.91	0.16
11-Sep-22	10.75	10.66	0.09	18-Sep-22	11.11	10.96	0.15

Note: Date = date of gauge observation; Gauge reading = observed flood level; Estimated water level = water level estimated from the statistical model; **Residuals**= difference between the observed and estimated water level: Predictive model = mathematical model from which the estimates were derived

Table 8a: Part of observed and forecasted water levels at ogbaru temporary station in 2012

Date	Ogbaru gauge readings in	Etimated water Level (m)	Predictive error	Date	Ogbaru gauge readings (m)	Estimated water Level (m)	Predictive error	Predictive Model.
1-Sep-2012	8.90	8.84	0.06	8-Sep-2012	9.47	9.64	-0.17	Y_{OG}=1.4127X_{ON} – 5.607 Y_{ON} = Estimated water level at Ogbaru, X_{ON} is measured water level at Onisha.
2-Sep-2012	9.05	9.05	0	9-Sep-2012	9.51	9.70	-0.19	
3-Sep-2012	9.15	9.19	-0.04	10-Sep-2012	9.56	9.77	-0.21	
4-Sep-2012	9.26	9.35	-0.09	11-Sep-2012	9.62	9.86	-0.24	
5-Sep-2012	9.31	9.42	-0.11	12-Sep-2012	10.08	9.91	0.17	
6-Sep-2012	9.32	9.43	-0.11	13-Sep-2012	10.09	10.03	0.06	
7-Sep-2012	9.36	9.49	-0.13	14-Sep-2012	10.14	10.05	0.09	

Note: Date = date of gauge observation; Gauge reading = observed flood level; Estimated water level = water level estimated from the statistical model; **Residuals**= difference between the observed and estimated water level: Predictive model = mathematical model from which the estimates were derived

Table 8b: Part of observed and forecasted water levels at Ogbaru temporary station in 2022

Date	Ogharu gauge readings in 2022(m)	Estimated water Level (m)	Residuals	Date	Ogbaru gauge readings in (m)	Estimated water Level (m)	Residuals
5-Sep-2022	8.85	8.84	-0.02	12-Sep-2022	9.42	9.64	-0.22
6-Sep-2022	9.00	9.05	0.04	13-Sep-2022	9.46	9.70	-0.24
7-Sep-2022	9.10	9.19	0.08	14-Sep-2022	9.51	9.77	-0.26
8-Sep-2022	9.21	9.35	0.14	15-Sep-2022	9.57	9.86	-0.29
9-Sep-2022	9.26	9.42	0.16	15-Sep-2022	10.02	9.91	0.11
10-Sep-2022	9.27	9.43	0.16	17-Sep-2022	10.03	10.03	0
11-Sep-2022	9.31	9.49	0.18	18-Sep-2022	10.08	10.05	0.03

Note: Date = date of gauge observation; Gauge reading = observed flood level; Estimated water level = water level estimated from the statistical model; Residuals = difference between the observed and estimated water level: Predictive model = mathematical model from which the estimates were derived

APPENDIX (A4)

Table 9a: Part of observed and estimated water levels at Ndokwa temporary station in 2012

Date	Ndokwa gauge readings in 2012 (m)	Estimated water Level (m)	**Residuals**	Date	Ndokwa gauge readings in 2012 (m)	Estimated water Level (m)	**Residuals**	Predictive Model
1-Sep-2012	8.19	8.11	0.07	8-Sep-2012	8.67	8.64	0.03	Y_{ND} 0.9182X_{OGB} – 0.0544 $Y_{nd}$is Estimated water level at Ndokwa, X_{OGB} is measured water level at Ogbaru
2-Sep-2012	8.34	8.25	0.08	9-Sep-2012	8.70	8.67	0.02	
3-Sep-2012	8.37	8.34	0.02	10-Sep-2012	8.75	8.72	0.02	
4-Sep-2012	8.47	8.44	0.02	11-Sep-2012	8.80	8.77	0.02	
5-Sep-2012	8.59	8.49	0.09	12-Sep-2012	8.90	9.2	-0.30	
6-Sep-2012	8.65	8.5	0.14	13-Sep-2012	9.28	9.21	0.06	
7-Sep-2012	8.67	8.53	0.13	14-Sep-2012	9.31	9.25	0.05	

Note: Date = date of gauge observation; Gauge reading = observed flood level; Estimated water level = water level estimated from the statistical model; **Residuals**= difference between the observed and estimated water level: Predictive model = mathematical model from which the estimates were derived

Table 9b: Part of observed and estimated water levels at Ndokwa temporary station in 2022

Date	Ndokwa gauge readings in 2022 (m)	Estimated water Level (m)	Residuals	Date	Ndokwa gauge readings in 2022 (m)	Estimated water Level (m)	Residuals
5-Sep-2022	8.09	8.11	-0.02	12-Sep-2022	8.61	8.64	-0.03
6-Sep-2022	8.23	8.25	-0.02	13-Sep-2022	8.74	8.67	0.07
7-Sep-2022	8.31	8.34	-0.03	14-Sep-2022	8.77	8.72	0.05
8-Sep-2022	8.48	8.44	0.04	15-Sep-2022	8.74	8.77	-0.03
9-Sep-2022	8.46	8.49	-0.03	15-Sep-2022	9.16	9.2	-0.04
10-Sep-2022	8.47	8.5	-0.03	17-Sep-2022	9.17	9.21	-0.04
11-Sep-2022	8.59	8.53	0.06	18-Sep-2022	9.28	9.25	0.03

Note: Date = date of gauge observation; Gauge reading = observed flood level; Estimated water level = water level estimated from the statistical model; Residuals = difference between the observed and estimated water level: Predictive model = mathematical model from which the estimates were derived

Table 10a: Part of Observed and estimated water levels at Patani temporary Gauging station in 2022

Date	Patani gauge readings in 2012 (m)	Estimated water Level (m)	Residuals	Date	Patani gauge readings in 2012 (m)	Estimated water Level (m)	Residuals	Predictive Model
1-Sep-2012	7.47	7.30	0.18	8-Sep-2012	7.96	7.78	0.17	$Y_{PA} = 1.0264X_{ND} - 1.1164$ Y_{PA} = Estimated water level Patani X_{ND} is measured water level at Ndokwa
2-Sep-2012	7.44	7.44	-0.00	9-Sep-2012	8.02	7.81	0.20	
3-Sep-2012	7.51	7.48	0.04	10-Sep-2012	8.03	7.86	0.16	
4-Sep-2012	7.63	7.58	0.05	11-Sep-2012	8.07	7.91	0.15	
5-Sep-2012	7.71	7.70	0.01	12-Sep-2012	8.11	8.01	0.09	
6-Sep-2012	7.8	7.76	0.04	13-Sep-2012	8.22	8.40	-0.18	
7-Sep-2012	7.9	7.78	0.12	14-Sep-2012	8.28	8.43	-0.15	

Note: Date = date of gauge observation; Gauge reading = observed flood level; Estimated water level = water level estimated from the statistical model; **Residuals**= difference between the observed and estimated water level: Predictive model = mathematical model from which the estimates were derived

APPENDIX (A5)

Table 10b: Part of Observed and estimated water levels at Patani temporary station in 2022

Date	Patan gauge readings in 2022 (m)	Estimated water Level (m)	Residuals	Date	Patani gauge readings in 2022 (m)	Estimated water Level (m)	Residuals
5-Sep-2022	7.45	7.30	0.15	12-Sep-2022	7.98	7.78	0.2
6-Sep-2022	7.40	7.44	-0.04	13-Sep-2022	8.02	7.81	0.21
7-Sep-2022	7.46	7.48	-0.02	14-Sep-2022	8.05	7.86	0.19
8-Sep-2022	7.55	7.58	-0.03	15-Sep-2022	8.03	7.91	0.12
9-Sep-2022	7.69	7.70	-0.01	15-Sep-2022	8.16	8.01	0.15
10-Sep-2022	7.82	7.76	0.06	17-Sep-2022	8.25	8.40	-0.15
11-Sep-2022	7.94	7.78	0.16	18-Sep-2022	8.33	8.43	-0.1

Note: Date = date of gauge observation; Gauge reading = observed flood level; Estimated water level = water level estimated from the statistical model; Residuals = difference between the observed and estimated water level: Predictive model = mathematical model from which the estimates were derived

Table 11a: Part of Observed and estimated water levels at Bomadi temporary station in 2012

Date	Bomadi gauge readings in 2012 (m)	Estimated water Level (m)	**Residuals**	Date	Bomadi gauge readings in 2012 (m)	Estimated water Level (m)	**Residuals**	Predictive Model
1-Sep-2012	7.75	7.76	-0.01	8-Sep-2012	8.14	8.16	-0.02	$Y_{BU} = 0.8272X_{PA} + 1.582$ Y_{PA} is estimated water at Burundi, X_{PA} is measured water level at Patani
2-Sep-2012	7.84	7.73	0.11	9-Sep-2012	8.15	8.21	-0.06	
3-Sep-2012	7.96	7.79	0.17	10-Sep-2012	8.2	8.22	-0.02	
4-Sep-2012	7.98	7.89	0.09	11-Sep-2012	8.27	8.25	0.02	
5-Sep-2012	8.04	7.95	0.09	12-Sep-2012	8.33	8.29	0.04	
6-Sep-2012	8.08	8.03	0.05	13-Sep-2012	8.43	8.38	0.05	
7-Sep-2012	8.11	8.11	0	14-Sep-2012	8.52	8.43	0.09	

Note: Date = date of gauge observation; Gauge reading = observed flood level; Estimated water level = water level estimated from the statistical model; Residuals= difference between the observed and estimated water level: Predictive model = mathematical model from which the estimates were derived

Table11b: Part of Observed and estimated water levels at Bomadi temporary station in 2022

Date	**Bomadi gauge readings in 2022 (m)**	**Estimated water Level (m)**	**Residuals**	**Date**	**Bomadi gauge readings in 2022 (m)**	**Estimated water Level (m)**	Residuals
5-Sep-2022	7.69	7.76	-0.07	12-Sep-2022	8.11	8.16	-0.05
6-Sep-2022	7.77	7.73	0.04	13-Sep-2022	8.17	8.21	-0.04
7-Sep-2022	7.98	7.79	0.19	14-Sep-2022	8.18	8.22	-0.04
8-Sep-2022	7.95	7.89	0.06	15-Sep-2022	8.25	8.25	0
9-Sep-2022	8.10	7.95	0.15	15-Sep-2022	8.36	8.29	0.07
10-Sep-2022	8.14	8.03	0.11	17-Sep-2022	8.45	8.38	0.07
11-Sep-2022	8.10	8.11	-0.01	18-Sep-2022	8.49	8.43	0.06

Note: Date = date of gauge observation; Gauge reading = observed flood level; Estimated water level = water level estimated from the statistical model; Residuals = difference between the observed and estimated water level: Predictive model = mathematical model from which the estimates were derived

APPENDIX (B1)

Table 4c: Part of observed and forecasted water levels at Ajeokuta station in 2018

Date	Ajeokuta gauge readings in 2012 (m)	Estimated water Level (m)	Residuals	Date	Ajeokuta gauge readings in 2012 (m)	Estimated water Level (m)	Residuals	Predictive Model
29-Aug-2018	9.58	9.6	-0.02	5-Sep-2018	10.05	9.95	0.1	$YA = 0.6955X_L+3.347$ (YA= estimated water level at Ajeokuta. XL= observed water level at Lokoja)
30-Aug-2018	9.5	9.69	-0.19	6-Sep-2018	10.08	9.96	0.12	
31-Aug-2018	9.58	9.79	-0.21	7-Sep-2018	10.14	10.01	0.13	
01-Sep-2018	9.73	9.81	-0.08	8-Sep-2018	10.18	10.07	0.11	
02-Sep-2018	9.81	9.87	-0.06	9-Sep-2018	10.22	10.13	0.09	
03-Sep-2018	9.91	9.9	0.01	10-Sep-2018	10.35	10.21	0.14	
04-Sep-2018	9.96	9.93	0.03	11-Sep-2018	10.41	10.3	0.11	
Note: Date = date of gauge observation; Gauge reading = observed flood level; Estimated water level = water level estimated from the statistical model; Residuals = difference between the observed and estimated water level: Predictive model = mathematical model from which the estimates were derived								

Table 5c: Part of observed and forecasted water levels at Idah station in 2018

Date	Idah Gauge Reading in 2012 (m)	Estimated Water level (m)	Residuals	Date	Idah Gauge Reading	Estimate	Residuals	Predictive Model
29-Aug-2018	9.18	9.08	0.1	5-Sep-2018	9.65	9.78	-0.13	$Y_{ID} = 1.4263X_A - 4.5519$ (Y_{ID}= estimated water level at Idah. X_A= observed water level at Ajeokuta
30-Aug-2018	9.3	9.04	0.26	6-Sep-2018	9.62	9.87	-0.25	
31-Aug-2018	9.4	9.14	0.26	7-Sep-2018	9.7	9.88	-0.18	
01-Sep-2018	9.41	9.31	0.1	8-Sep-2018	9.83	9.94	-0.11	
02-Sep-2018	9.47	9.42	0.05	9-Sep-2018	9.92	9.99	-0.07	
03-Sep-2018	9.57	9.55	0.02	10-Sep-2018	10.03	10.15	-0.12	
04-Sep-2018	9.61	9.69	-0.08	11-Sep-2018	10.15	10.24	-0.09	
Note: Date = date of gauge observation; Gauge reading = observed flood level; Estimated water level = water level estimated from the statistical model; Residuals = difference between the observed and estimated water level: Predictive model = mathematical model from which the estimates were derived								

Table 6c: Part of observed and forecasted water levels at Illushi station in 2018

Date	IllushiGauge Reading (m)	Estimated water level (m)	Residuals	Date	Illushi Gauge Reading	Estimated water level	Residuals	Predictive model
29-Aug-2018	9.18	9.12	0.06	5-Sep-2018	9.65	9.62	0.03	Y_{IL}= I,0025X_{ID} -- 0.0467. (Y_{IL}= Estimated water level at Illushi, X_{ID}= Measured water Level at Idah
30-Aug-2018	9.3	9.24	0.06	6-Sep-2018	9.62	9.64	-0.02	
31-Aug-2018	9.4	9.39	0.01	7-Sep-2018	9.7	9.71	-0.01	
01-Sep-2018	9.41	9.42	-0.01	8-Sep-2018	9.83	9.79	0.04	
02-Sep-2018	9.47	9.5	-0.03	9-Sep-2018	9.92	9.88	0.04	
03-Sep-2018	9.57	9.55	0.02	10-Sep-2018	10.03	10	0.03	
04-Sep-2018	9.61	9.59	0.02	11-Sep-2018	10.15	10.12	0.03	
Note: Date = date of gauge observation; Gauge reading = observed flood level; Estimated water level = water level estimated from the statistical model; **Residuals**difference between the observed and estimated water level: Predictive model = mathematical model from which the estimates were derived								

APPENDIX (B2)

Table 7c: Part of observed and forecasted water levels at Onisha station in 2018

Date	Ogbaru gauge readings in	Etimated water Level (m)	Predictive error	Date	Ogbaru gauge readings (m)	Estimated water Level (m)	Predictive error	Predictive Model.
29-Aug-2018	8.87	8.84	0.03	5-Sep-2018	9.46	9.64	-0.18	Y_{OG}=1.4127X_{ON} – 5.607 Y_{ON} = Estimated water level at Ogbaru,, X_{ON} is measured water level at Onisha.
30-Aug-2018	9.01	9.05	-0.04	6-Sep-2018	9.57	9.7	-0.13	
31-Aug-2018	9.16	9.19	-0.03	7-Sep-2018	9.59	9.77	-0.18	
01-Sep-2018	9.29	9.35	-0.06	8-Sep-2018	9.56	9.86	-0.3	
02-Sep-2018	9.36	9.42	-0.06	9-Sep-2018	10.03	9.91	0.12	
03-Sep-2018	9.24	9.43	-0.19	10-Sep-2018	10.08	10.03	0.05	
04-Sep-2018	9.36	9.49	-0.13	11-Sep-2018	10.13	10.05	0.08	
Note: Date = date of gauge observation; Gauge reading = observed flood level; Estimated water level = water level estimated from the statistical model; **Residuals**= difference between the observed and estimated water level: Predictive model = mathematical model from which the estimates were derived								

Table 8c: Part of observed and forecasted water levels at Ogbaru station in 2018

`Date	Onisha Gauge Reading (m)	Estimated Water level. (m)	Residuals	Date	Onisha Gauge Reading (m)	Estimated Water level. (m)	Residuals	Predictive model
29-Aug-18	10.26	10.42	-0.16	05-Sep-18	10.81	10.72	0.09	YO N = 0.5223XIL + 5.6696 Y_{ON} = Estimated water level at Onisha., X_{IL} = Measured Water level at Illushi
30-Aug-18	10.42	10.52	-0.1	06-Sep-18	10.78	10.75	0.03	
31-Aug-18	10.47	10.61	-0.14	07-Sep-18	10.86	10.79	0.07	
01-Sep-18	10.56	10.61	-0.05	08-Sep-18	11.01	10.85	0.16	
02-Sep-18	10.59	10.62	-0.03	09-Sep-18	11.04	10.89	0.15	
03-Sep-18	10.73	10.64	0.09	10-Sep-18	11.06	10.91	0.15	
04-Sep-18	10.69	10.66	0.03	11-Sep-18	11.1	10.96	0.14	
Note: Date = date of gauge observation; Gauge reading = observed flood level; Estimated water level = water level estimated from the statistical model; **Residuals=** difference between the observed and estimated water level: Predictive model = mathematical model from which the estimates were derived								

Table 9c: Part of observed and forecasted water levels at Ndokwa station in 2018

Date	Ndokwa gauge readings in 2012 (m)	Estimated water Level (m)	**Residuals**	Date	Ndokwa gauge readings in 2012 (m)	Estimated water Level (m)	**Residuals**	Predictive Model
29-Aug-2018	8.08	8.11	-0.03	5-Sep-2018	8.63	8.64	-0.01	Y_{ND} 0.9182X_{OGB} – 0.0544 $Y_{nd}$is Estimated water level at Ndokwa, X_{OGB} is measured water level at Ogbaru
30-Aug-2018	8.21	8.25	-0.04	6-Sep-2018	8.73	8.67	0.06	
31-Aug-2018	8.35	8.34	0.01	7-Sep-2018	8.75	8.72	0.03	
01-Sep-2018	8.47	8.44	0.03	8-Sep-2018	8.71	8.77	-0.06	
02-Sep-2018	8.54	8.49	0.05	9-Sep-2018	9.15	9.2	-0.05	
03-Sep-2018	8.42	8.5	-0.08	10-Sep-2018	9.2	9.21	-0.01	
04-Sep-2018	8.53	8.53	0	11-Sep-2018	9.24	9.25	-0.01	
Note: Date = date of gauge observation; Gauge reading = observed flood level; Estimated water level = water level estimated from the statistical model; **Residuals**= difference between the observed and estimated water level: Predictive model = mathematical model from which the estimates were derived								

APPENDIX (B3)

Table 10c: Part of observed and forecasted water levels at Patani station in 2018

Date	Patan gauge readings in 2022 (m)	Estimated water Level (m)	Residuals	Date	Patani gauge readings in 2022 (m)	Estimated water Level (m)	Residuals
29-Aug-2018	7.54	7.3	0.24	5-Sep-2018	8.04	7.78	0.26
30-Aug-2018	7.67	7.44	0.23	6-Sep-2018	8.01	7.81	0.2
31-Aug-2018	7.7	7.48	0.22	7-Sep-2018	8.08	7.86	0.22
01-Sep-2018	7.77	7.58	0.19	8-Sep-2018	8.28	7.91	0.37
02-Sep-2018	7.85	7.7	0.15	9-Sep-2018	8.33	8.01	0.32
03-Sep-2018	8.04	7.76	0.28	10-Sep-2018	8.35	8.4	-0.05
04-Sep-2018	8.02	7.78	0.24	11-Sep-2018	8.56	8.43	0.13
Note: Date = date of gauge observation; Gauge reading = observed flood level; Estimated water level = water level estimated from the statistical model; Residuals = difference between the observed and estimated water level: Predictive model = mathematical model from which the estimates were derived							

Table 11c: Part of observed and forecasted water levels at Burundi station in 2018

Date	Bomadi gauge readings in 2012 (m)	Estimated water Level (m)	**Residuals**	Date	Burundi gauge readings in 2012 (m)	Estimated water Level (m)	**Residuals**	Predictive Model
29-Aug-2018	7.82	7.76	0.06	8-Sep-2012	8.19	8.16	0.03	Y_{BU} =0.8272X_{PA} + 1.582 Y_{PA} is estimated water at Burundi, X_{PA} is measured water level at Patani
30-Aug-2018	7.8	7.73	0.07	9-Sep-2012	8.19	8.21	-0.02	
31-Aug-2018	7.77	7.79	-0.02	10-Sep-2012	8.24	8.22	0.02	
01-Sep-2018	7.92	7.89	0.03	11-Sep-2012	8.27	8.25	0.02	
02-Sep-2018	7.89	7.95	-0.06	12-Sep-2012	8.26	8.29	-0.03	
03-Sep-2018	7.97	8.03	-0.06	13-Sep-2012	8.36	8.38	-0.02	
04-Sep-2018	8.12	8.11	0.01	14-Sep-2012	8.46	8.43	0.03	
Note: Date = date of gauge observation; Gauge reading = observed flood level; Estimated water level = water level estimated from the statistical model; Residuals= difference between the observed and estimated water level: Predictive model = mathematical model from which the estimates were derived								